HOST-MICROBE INTERACTIONS

Bacterial D-amino acids suppress sinonasal innate immunity through sweet taste receptors in solitary chemosensory cells

Robert J. Lee,[1,2]* Benjamin M. Hariri,[1] Derek B. McMahon,[1] Bei Chen,[1] Laurel Doghramji,[1] Nithin D. Adappa,[1] James N. Palmer,[1] David W. Kennedy,[1] Peihua Jiang,[3] Robert F. Margolskee,[3] Noam A. Cohen[1,3,4]*

In the upper respiratory epithelium, bitter and sweet taste receptors present in solitary chemosensory cells influence antimicrobial innate immune defense responses. Whereas activation of bitter taste receptors (T2Rs) stimulates surrounding epithelial cells to release antimicrobial peptides, activation of the sweet taste receptor (T1R) in the same cells inhibits this response. This mechanism is thought to control the magnitude of antimicrobial peptide release based on the sugar content of airway surface liquid. We hypothesized that D-amino acids, which are produced by various bacteria and activate T1R in taste receptor cells in the mouth, may also activate T1R in the airway. We showed that both the T1R2 and T1R3 subunits of the sweet taste receptor (T1R2/3) were present in the same chemosensory cells of primary human sinonasal epithelial cultures. Respiratory isolates of *Staphylococcus* species, but not *Pseudomonas aeruginosa*, produced at least two D-amino acids that activate the sweet taste receptor. In addition to inhibiting *P. aeruginosa* biofilm formation, D-amino acids derived from *Staphylococcus* inhibited T2R-mediated signaling and defensin secretion in sinonasal cells by activating T1R2/3. D-Amino acid–mediated activation of T1R2/3 also enhanced epithelial cell death during challenge with *Staphylococcus aureus* in the presence of the bitter receptor–activating compound denatonium benzoate. These data establish a potential mechanism for interkingdom signaling in the airway mediated by bacterial D-amino acids and the mammalian sweet taste receptor in airway chemosensory cells.

INTRODUCTION

The nose and sinuses are the front line of respiratory defense (*1*). When sinonasal immunity fails, it can result in chronic rhinosinusitis (CRS), a debilitating disease affecting >10% of Americans and accounting for ~$8 billion of annual direct health care costs (*2–4*). First-line therapy for bacterial rhinosinusitis involves antibiotics; rhinosinusitis accounts for one in five antibiotic prescriptions for adults in the United States, making it a major contributor to the rising crisis of antibiotic resistance (*5–7*). There is a critical need to better understand the regulation of endogenous sinonasal immune responses to identify novel therapeutic targets that could treat CRS without the use of antibiotics to avoid selective pressures for resistance. We previously showed that sinonasal solitary chemosensory cells (SCCs), a recently identified cell type in the upper airway, stimulate secretion of antimicrobial peptides (AMPs) through bitter taste receptors (T2Rs) (*8*). T2Rs, originally identified on the tongue (*9*, *10*), are found in many tissues throughout the body (*11–13*). T2Rs are activated by toxic plant products, such as alkaloids, as well as bitter bacterial products, such as acyl-homoserine lactone (AHL) quorum-sensing molecules (*8*, *13–18*). SCCs, a specific cell type found at a frequency of ~1:100 in the upper airway and which expresses both bitter and sweet taste receptors, were first described in fish (*19*) and later in alligators (*20*), rodents (*21–23*), and humans (*8*, *24*). SCCs are defined by expression of taste-signaling components, including bitter receptors (T2Rs), sweet receptors (T1R2/3), and Gα-gustducin (*8*, *21–24*). Acti-

vation of T2Rs in human sinonasal SCCs stimulates propagation of a calcium wave to the surrounding epithelial cells, causing release of AMPs (including β-defensins) that kill bacteria (*8*).

This mechanism is inhibited by activation of sweet taste receptors (T1Rs) (*25*), which are localized within the same SCCs as the bitter taste receptors (*8*). SCC responses stimulated by the bitter T2R agonist denatonium are blocked in a dose-dependent fashion by sugars such as glucose and sucrose, as well as the nonmetabolizable artificial sweetener sucralose (*8*). This inhibition is blocked by the T1R2/3 (T1R receptor containing T1R2 and T1R3 subunits) antagonists lactisole (*26–28*) and amiloride (*29*) but not by inhibitors of glucose transporters (*8*). Glucose tonically leaks across the epithelium into the airway surface liquid (ASL) through paracellular pathways, but reuptake through apical glucose transporters in the healthy state maintains ASL glucose at around 0.5 mM or less, which is about 10-fold less than fasting serum concentration (*30–32*). However, such low glucose concentrations are nonetheless sufficient to partially activate T1R2/3 in human nasal SCCs (*8*). We have hypothesized that T1R2/3 acts as a rheostat to control the magnitude of the AMP response depending on ASL glucose concentrations, desensitizing SCC T2Rs to bitter compounds during colonization. This desensitization would be relieved when bacterial numbers increase enough to cause depletion of ASL glucose through bacterial glucose consumption, signaling the onset of a bona fide infection (*8*).

Although this hypothesis requires further validation, another mechanism by which airway T1R2/3 receptors may be activated is through bacterial production of D-amino acids, several of which activate the sweet taste receptor (*26*, *33*). Life has evolved to predominantly use L-amino acids as protein building blocks, but bacteria produce a diverse array of D-amino acids used as cell wall structural components and possibly intercellular signals. The racemase activity of bacteria and their resulting ability to interconvert and metabolize both D- and L-amino acids

[1]Department of Otorhinolaryngology—Head and Neck Surgery, University of Pennsylvania Perelman School of Medicine, Philadelphia, PA 19104, USA. [2]Department of Physiology, University of Pennsylvania Perelman School of Medicine, Philadelphia, PA 19104, USA. [3]Monell Chemical Senses Center, Philadelphia, PA 19104, USA. [4]Philadelphia Veterans Affairs Medical Center Surgical Service, Philadelphia, PA 19104, USA.
*Corresponding author. Email: rjl@mail.med.upenn.edu (R.J.L.); cohenn@uphs.upenn.edu (N.A.C.)

have been proposed to be responsible for maintaining the relatively low D-amino acid/L-amino acid ratio found on Earth (34). The Gram-negative bacterium *Vibrio cholera* and the Gram-positive bacterium *Bacillus subtilis* produce D-amino acids, which may reduce peptido-glycan synthesis and influence cell wall remodeling (35).

D-Amino acids may stimulate biofilm disassembly in *B. subtilis* (36) and inhibit biofilm formation of *Pseudomonas aeruginosa* (37, 38), *Staphylococcus aureus* (39, 40), and *Staphylococcus epidermidis* (41) as well as cause dispersal or detachment of cells from single-species and multispecies biofilms containing *P. aeruginosa* (42), *S. epidermidis* (41), or *S. aureus* (43, 44). D-Amino acids may inhibit adhesion of bacterial cells to one another (45, 46). However, other studies starkly conflict with these results and suggest that D-amino acids at 1 mM do not inhibit biofilm growth in *S. aureus*, *B. subtilis*, or *S. epidermidis* (47). Effects of D-amino acids on *B. subtilis* may be simply due to toxic effects of inhibition of protein synthesis (48). Others have reported that mixtures of D-amino acids (49) or combinations of D-amino acids with antibiotics (50) may be more effective against biofilm formation than individual D-amino acids. Interpretation of these studies is complicated because of differences in strains, biofilm assays (for example, microtiter plate versus flow cell), and the dosage of specific D-amino acids used (51).

Regardless of the controversy over the mechanism(s) of action of D-amino acids on the bacteria themselves, both Gram-negative and Gram-positive bacteria produce various D-amino acids at relatively high concentrations (in the high-micromolar to low-millimolar range) (35, 36, 52). This range is predicted to be sufficient to activate the sweet taste receptor (33, 53) on the airway epithelial SCCs that produce T1R2/3. We hypothesize that certain D-amino acids produced by bacteria may play an important role in host-pathogen interactions in the sinonasal cavity by activating the sweet taste receptor in SCCs, and thus, we sought to study the effects of sweet receptor–activating D-amino acids on upper respiratory epithelial cells and on the physiology of respiratory bacteria. Our goal was to test the effects of bacterially produced D-amino acids on airway epithelial innate immune responses to understand how they may influence host-pathogen interactions in the upper respiratory tract.

RESULTS

Sinonasal SCCs produce the T1R2 and T1R3 subunits of the sweet taste receptor

The canonical sweet taste receptor is composed of Tas1R2 (T1R2) and Tas1R3 (T1R3) subunits (54). A closely related subunit, Tas1R1 (T1R1), also combines with T1R3 to form the umami receptor (Fig. 1, A and B). These proteins are found only in vertebrates and are members of the class C family of heterotrimeric guanine nucleotide-binding protein–coupled receptors (GPCRs), which also includes metabotropic glutamate receptors as well as several receptors that detect amino acids and small peptides, including V2R pheromone receptors (Fig. 1A, fig. S1, and table S1) (54). The evolution of T1Rs from ancestral receptors for amino acids and peptides likely explains the reactivity of these receptors to certain amino acid isoforms. Typically, the umami receptor (T1R1/3, formed by the association of T1R1 and T1R3 subunits) detects the L-isomer (savory) amino acids, and the sweet receptor (T1R2/3, formed by the association of T1R2 and T1R3) detects certain D-isomers of amino acids in addition to various sugars, including sucrose, glucose, and fructose (55), as well as several known sweet peptides, such as monellin (56).

When primary human sinonasal cells were grown in air-liquid interface (ALI) cultures, these cultures contained SCCs, which were
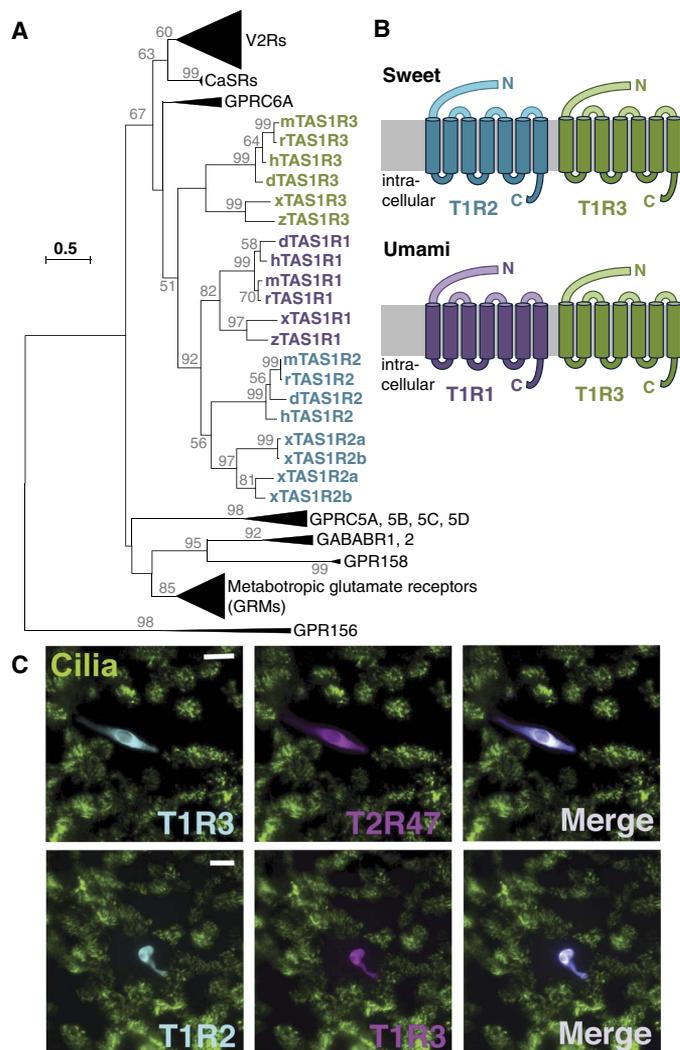

Fig. 1. Evolutionary relationship of sweet and umami taste receptor subunits. (**A**) Condensed evolutionary tree showing mouse (m), rat (r), human (h), dog (d), frog (x), and zebra fish (z) Tas1R1 (purple), Tas1R2 (blue), and Tas1R3 (green) subunits within the class C GPCR family. This family also includes the V2R pheromone receptors, the calcium-sensing receptors (CaSRs), the metabotropic glutamate receptors, and the other GPCRs indicated in black text. The full tree is shown in fig. S1. (**B**) Tas1R3 (T1R3) combines with Tas1R2 (T1R2) or Tas1R1 (T1R1) to form the sweet or umami receptors, respectively. (**C**) Sinonasal SCCs in human primary sinonasal ALI cultures produce both T1R2 and T1R3 sweet taste receptor subunits. Images are representative of three independent experiments using ALIs from three individual patients. Scale bars, 20 μm.

identified by morphological criteria and production of both bitter and sweet taste receptors, as previously described in mouse (57) and human (8, 58). SCCs are found at an approximate frequency of about 1 in 100 cells in the mouse sinonasal epithelium (57). Although we previously reported that human SCCs produce both T1R2 and T1R3 along with the bitter taste receptor T2R47, we did not determine whether the same SCC produces both T1R2 and T1R3 together, which would be required for formation of the canonical sweet taste receptor, T1R2/3. Here, we used direct labeling of SCCs using antibodies recognizing both T1R2 and T1R3 subunits. All SCCs observed in these cultures produced both T1R2 and T1R3 (Fig. 1C and fig. S2). We did not observe any SCCs in which only T1R2 or T1R3 was present alone. When costaining was

done with T2R47 and T1R2 or T1R3, T2R47-positive cells were always observed to produce T1R2 or T1R3. On the basis of these and our previous observations from human SCCs (8) and other observations of mouse SCCs (17, 21, 57), we conclude that sinonasal SCCs produce both bitter taste receptors (such as T2R47) and both subunits of the T1R2/3 receptor. However, our data do not rule out the existence of a distinct subset of SCCs that expresses neither T1R2 nor T1R3.

T1R2/3-activating D-amino acids are produced by bacteria cultured from the human sinonasal cavity

We hypothesized that D-amino acids produced by bacteria may impair the ability of SCCs to stimulate innate immune responses by activating T1R2/3. Note that, in this study, we are not measuring "sweetness," which is a complex gustatory sensation, but rather looking at activation of the T1R2/3 receptor. Thus, instead of referring to these amino acids as "sweet," as in many psychophysics studies (59, 60), we refer to them here as "T1R2/3-activating" amino acids, as demonstrated in previous molecular experiments (26, 33). We measured the abundance of several D-amino acids known to activate the T1R2/3 receptor [D-Ile, D-Phe, and D-Leu (26, 33)] in bacterial cultures grown from human sinonasal swabs from CRS patients. Not all D-amino acids activate the sweet taste receptor; an example is D-proline, which does not activate T1R2/3 and is perceived as bitter (61). Thus, we specifically focused on D-Ile, D-Phe, and D-Leu, which are known to activate T1R2/3. Because these samples came from human patients, they were not strictly single-species cultures, so we determined the predominant microorganisms present in each culture. These included S. aureus, coagulase-negative Staphylococcus (likely primarily S. epidermidis), P. aeruginosa, and Aspergillus fumigatus. We classified these cultures by the predominant species present in the culture, but other species were also present in each culture at lower abundance. Cultures in which either S. aureus or coagulase-negative Staphylococcus was predominant contained D-Phe and D-Leu, whereas cultures in which P. aeruginosa or A. fumigatus was predominant did not (Fig. 2A).

D-Amino acids reduce P. aeruginosa biofilm formation and swarming

To determine whether the D-amino acids present in clinical microbiologic cultures might affect the growth of bacteria, we grew wild-type P. aeruginosa strain PAO1 and methicillin-resistant S. aureus (MRSA) strain M2 in filter-sterilized conditioned medium (CM) from sinonasal clinical cultures. CM from cultures in which S. aureus was predominant, but not CM from cultures in which P. aeruginosa was predominant, reduced biofilm formation by P. aeruginosa strain PAO1 (Fig. 2B). MRSA M2 biofilm formation was not affected by CM from either S. aureus–predominant or P. aeruginosa–predominant cultures. When a clinical MRSA strain and P. aeruginosa PAO1 biofilms were grown in a medium supplemented with varying concentrations of D-Phe, D-Leu, and D-Tyr [another D-amino acid previously shown to be produced by P. aeruginosa and activate T1R2/3 (35)], we found that P. aeruginosa PAO1 exhibited a 10-fold lower median inhibitory concentration (IC$_{50}$) than did MRSA as well as a higher maximum inhibition of biofilm formation (Fig. 2C), suggesting that P. aeruginosa PAO1 has a greater sensitivity to the biofilm inhibitory effects of D-amino acids produced by Staphylococcus species. L-Amino acids supplemented at the same concentrations had no effect on biofilm formation (Fig. 2C). Whether these concentrations translate to in vivo D-amino acid production remains to be determined.

We noted that planktonic cultures of P. aeruginosa [wild-type PAO1 or American Type Culture Collection (ATCC) 27853] grown in the

presence of two T1R2/3-activating D-amino acids (D-Phe + D-Leu) were less blue-green than when cultured in the absence of these D-amino acids (Fig. 3A). This was due at least in part to a reduction in the production of pyocyanin, a secreted toxic secondary metabolite (Fig. 3, B and C).
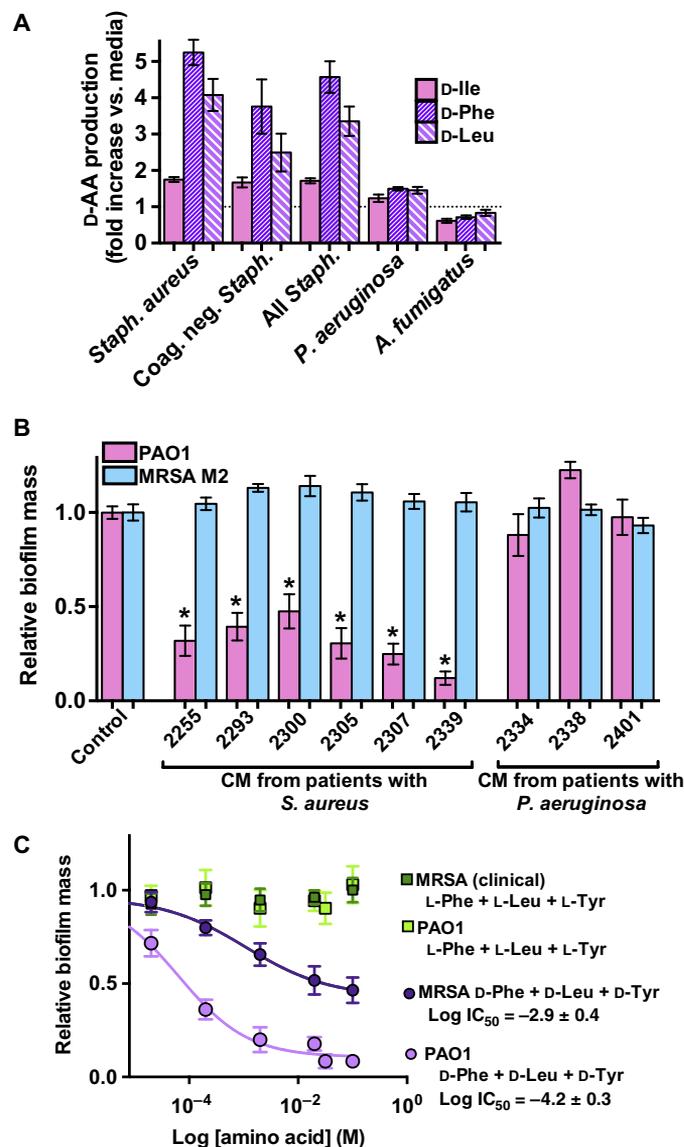

Fig. 2. Bacteria and sweet D-amino acids in clinical sinonasal microbiologic cultures and effects on biofilm formation. (**A**) Fold increases in D-Phe, D-Leu, and D-Ile from sinonasal microorganism CM compared to starting medium. $n = 5$ to 12 independent culture samples for each condition tested separately for each D-amino acid. (**B**) Biofilm formation by P. aeruginosa strain PAO1 and MRSA strain M2 in the presence of CM from the indicated patient samples. $n = 6$ to 10 independent experiments for each condition and concentration; each single experiment represents an average of >8 wells of a 96-well plate. *$P < 0.05$ by one-way analysis of variance (ANOVA), Dunnett's posttest comparing values to strain-specific control. (**C**) Dose-dependent effects of L-Phe + L-Leu + L-Tyr or D-Phe + D-Leu + D-Tyr on P. aeruginosa PAO1 and MRSA biofilm formation. Because of the poor solubility of L-Tyr and D-Tyr, the maximum concentration of L-Tyr or D-Tyr in these experiments was 0.1 mM. For amino acid concentrations indicated as greater than 0.1 mM on the graph, the indicated concentration refers to the concentration of L-Phe or D-Phe and L-Leu or D-Leu, with L-Tyr or D-Tyr at 0.1 mM. $n = 6$ to 10 independent experiments for each condition and concentration; each single experiment represents an average of >8 wells of a 96-well plate.
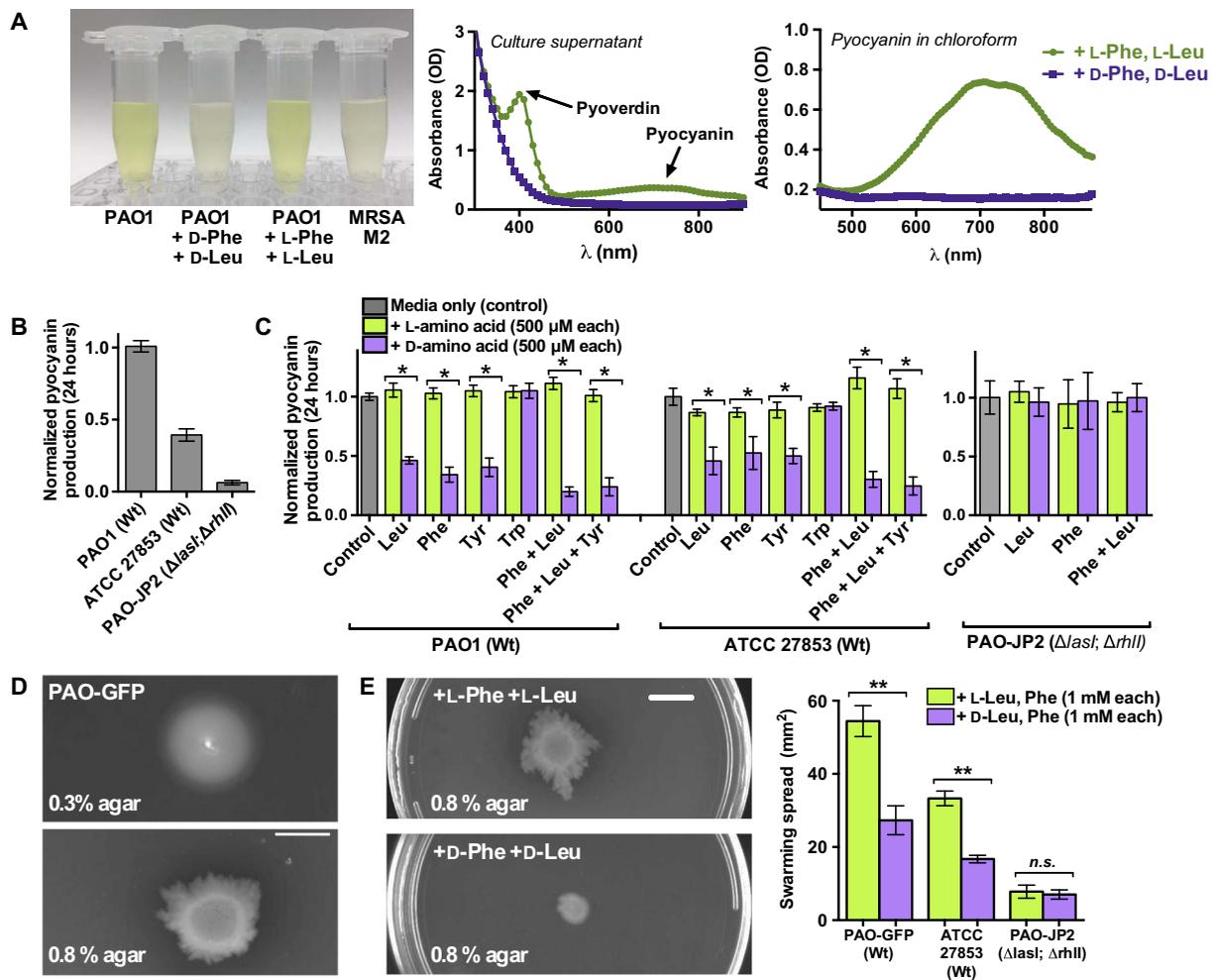
Fig. 3. Effects of sweet D-amino acids on *P. aeruginosa* pyocyanin production and swarming. (**A**) Color of PAO1 supernatant in the presence of L- or D-amino acids and representative absorption spectra of supernatant or chloroform-extracted pyocyanin. *n* = 3 to 10 independent experiments per strain per condition; each experiment averaged three suspension cultures. (**B**) Bar graph of relative pyocyanin abundance in *P. aeruginosa* strains. *n* = 3 independent experiments for each strain; each single experiment averaged three suspension cultures. Wt, wild-type. (**C**) Quantification of relative pyocyanin abundance in strains PAO1 and ATCC 27853, which are biofilm-competent, and PAO-JP2, which cannot form biofilms. *n* = 3 to 10 independent experiments per strain per condition; each single experiment averaged three suspension cultures. (**D**) Morphology of PAO-GFP colonies under conditions that favor swimming (0.3% agar) or swarming (0.8% agar). Scale bar, 1 cm. (**E**) Morphology of PAO-GFP colonies under swarming conditions and quantification of swarming in the presence of the indicated amino acids. Scale bar, 1 cm. Graphs show means ± SEM with *$P < 0.05$ and **$P < 0.01$ (one-way ANOVA, Bonferroni posttest comparing bracketed groups). *n* = 5 independent experiments for each condition per strain; each experiment averaged three plates.

As a control, a strain deficient in AHL quorum sensing (PAO-JP2; Δ*lasI*, Δ*rhlI*), which produces very little pyocyanin at baseline (Fig. 3B), was unaffected by the presence of D-Phe or D-Leu (Fig. 3C). Because biofilm formation and pyocyanin production are under the control of the AHL quorum-sensing system, we also tested swarming motility in *Pseudomonas*, which is likewise controlled by quorum sensing. Swarming is important for bacterial spreading and biofilm formation (*62*) and requires flagellar function and rhamnolipid production (*62*, *63*). Swarming is evidenced by a characteristic irregular radiation of cells from a spot on semisolid high-density agar plates that mimic gelatinous viscous surfaces like the mucosal membrane (*62*). In contrast, swimming on low-agar plates, which reflects random twitching motility, results in a more even diffusive colony spread (Fig. 3D). Swarming was markedly inhibited in the presence of D-Phe and D-Leu but not in the presence of L-Phe and L-Leu for PAO–green fluorescent protein (GFP) (a derivative of PAO1) and ATCC 27853. The presence of either L- or D-amino acids did not affect swarming of PAO-JP2 (Fig. 3E). The above data support some

role of D-amino acids in the inhibition of quorum sensing and biofilm formation in vitro.

Because D-amino acids have been implicated in bacterial biofilm dispersal and cell wall remodeling of some bacteria, we tested the effects of T1R2/3-activating D-amino acids on dispersion of microcolonies of PAO-GFP grown on glass coverslips (fig. S3), low-salt sensitivity of PAO1 (fig. S4), and antibiotic resistance of PAO-GFP and ATCC 27853 (fig. S5). We observed no differences in any of these parameters between bacteria exposed to D- or L-amino acids. Our negative data suggest that these T1R2/3-activating D-amino acids do not affect *P. aeruginosa* dispersion or cell wall integrity.

T1R2/3-activating D-amino acids affect innate immune responses of sinonasal cells by modulating the T1R2/3 receptor

We next tested the effects of the T1R2/3-activating D-amino acids D-Phe and D-Leu on host cell innate immune responses. We examined the

Fig. 4. Effects of D-amino acids on SCC T2R Ca²⁺ responses. (**A**) Ca²⁺ responses of SCCs treated with denatonium (10 mM applied apically; abbreviated 10 D) in the presence or absence of glucose (Glc) ± lactisole (Lact) or GA2. Traces shown are the average (±SEM) of multiple experiments (*n* = 6 to 10); each experiment was performed on a single ALI culture from a separate individual patients (thus, cells from 6 to 10 patients were examined per condition). (**B**) Calcium responses in the presence of D-Leu or L-Leu (2 mM; top) and D-Phe or L-Phe (2 mM; bottom) ± lactisole. *n* = 5 to 8 experiments, each experiment was performed on a single ALI from a separate individual patient (thus, cells from five to eight patients were examined per condition). (**C**) Summary of peak Fluo-4 *F/F₀* values for data shown in (A) and (B). Pound symbols (#) indicate significance compared with control (denatonium only); asterisks denote significance between brackets; #*P* < 0.05, *P* < 0.05, ##*P* < 0.01, and **P* < 0.01 by one-way ANOVA with Bonferroni posttest. (**D**) β-Defensin secreted into ASL after treatment with the indicated combinations of denatonium (Denat), glucose (Glc), gymnemic acis (GA2), sucralose (S), and lactisole (Lact) in phosphate-buffered saline (PBS). *n* = 4 to 6 ALI cultures per condition, each from a separate individual patient; *P* < 0.05 and **P* < 0.01 compared with PBS (unstimulated control) by one-way ANOVA with Dunnett's posttest.
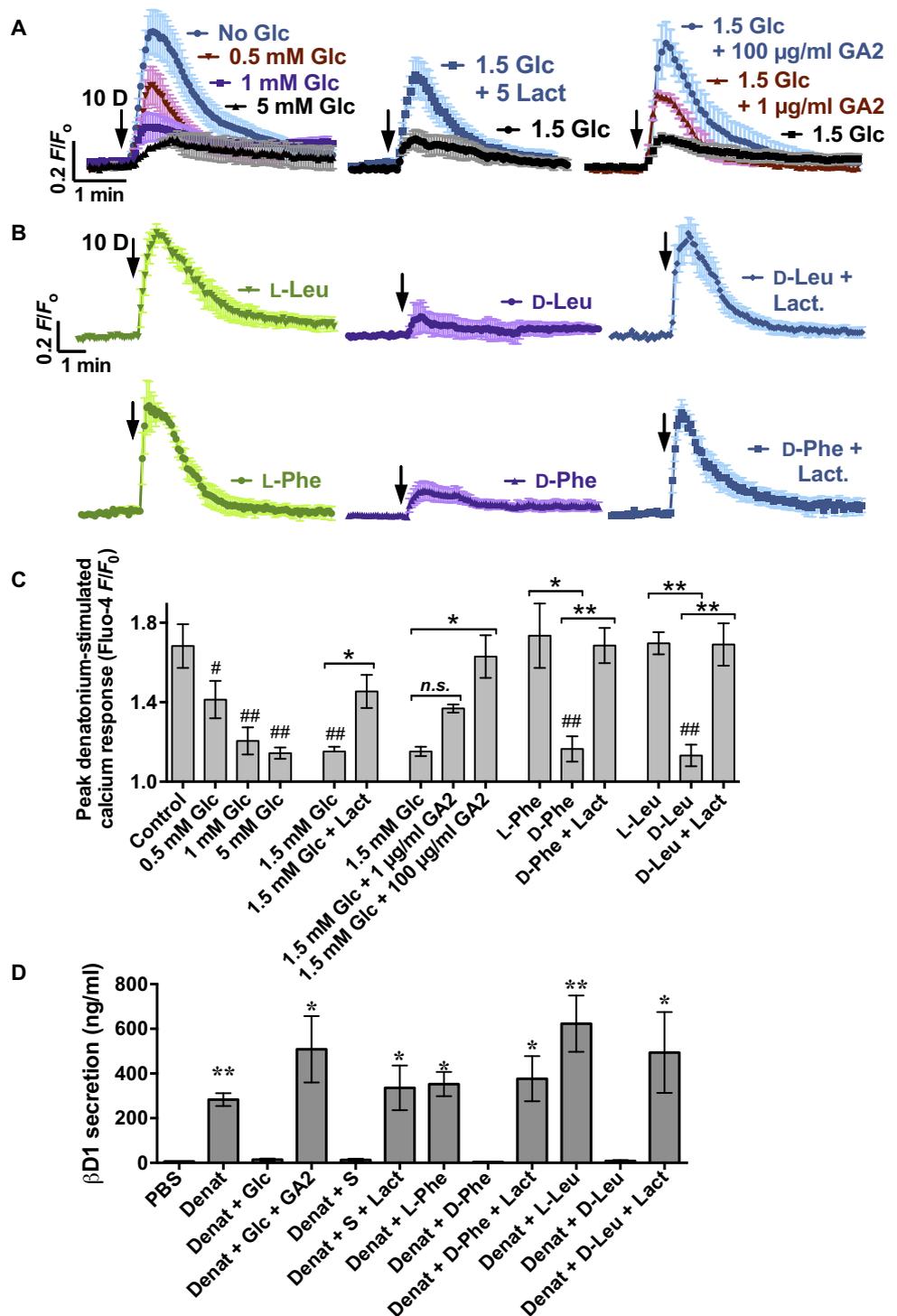
effects of the D- and L-isomers of Phe and Leu on T2R-mediated calcium responses of human SCCs grown in ALI cultures. This culturing method is a standard in vitro model of the airway epithelium that mimics the morphology of the in vivo airway epithelium and includes ciliated cells, goblet cells, and SCCs (8, 14, 64–66). ALI cultures grown at physiological concentrations of basolateral glucose (5 mM or 90 mg/dl) produce ASL containing ~0.3 to 0.5 mM glucose, which is similar to the concentration of glucose in control nasal fluid samples (8). This glucose concentration, which results from transepithelial leak of basolateral glucose through paracellular pathways balanced by cellular reuptake of glucose through apical glucose transporters (GLUTs) (30, 31), is sufficient to slightly attenuate T2R Ca²⁺ responses in SCCs (8). For this reason, cultures were thoroughly washed immediately before experiments to remove any residual ASL glucose that may influence the cells.

As previously reported (8), the T2R agonist denatonium benzoate stimulated Ca²⁺ responses from SCCs that were inhibited dose-dependently by the presence of apical glucose (0.5 to 5 mM). The sweet taste receptor antagonists—lactisole (27, 28) and gymnemic acid (67, 68)—blocked glucose-mediated inhibition of SCC calcium responses (Fig. 4A). When SCCs were exposed to D-Leu or D-Phe, but not L-Leu or L-Phe, they likewise exhibited reduced denatonium-stimulated Ca²⁺ responses (Fig. 4B) that were also reversed by lactisole. We previously showed that these SCC Ca²⁺ responses (Fig. 4C) drive AMP secretion from the surrounding epithelial cells in response to T2R receptor stimulation (8). The D-Leu and D-Phe suppression of denatonium-induced

Ca^{2+} signaling suggests that D-Leu and D-Phe have effects on SCC signal transduction upstream of AMP release, as we previously reported for sugars and artificial sweeteners acting through the sweet taste receptor (8). The decrease in SCC Ca^{2+} signaling elicited by D-Leu and D-Phe also resulted in reduced β-defensin 1 (βD1) secretion, which was likewise reversed by lactisole (Fig. 4D). D-Phe and D-Leu also reduced Ca^{2+} responses in cultured nasal septum ALI cultures from wild-type but not T1R3 knockout mice (fig. S6), supporting the idea that this reduction occurs through the sweet taste receptor.

We next tested the hypothesis that T1R2/3-activating D-amino acids impair epithelial defense by examining the effects of MRSA bacterial coculture on cell viability in sinonasal ALI cultures in the presence and absence of these secreted D-amino acids. We examined host cell death after incubation of the cells with the laboratory strain MRSA M2, by determining the proportion of live and dead cell staining with Syto9, a fluorescent compound that labels the nuclei of both live and dead cells, and propidium iodide (PI), a fluorescent compound that labels the nuclei only of dead or dying cells. We estimated the number of live and dead cells by measuring the relative areas of Syto9 and PI staining, respectively, using fluorescence microscopy. Representative images are shown (Fig. 5A) with quantification of staining (Fig. 5B). In the absence of bacteria, ALI cultures exhibited no detectable cell death (Fig. 5A, upper left), evidenced by a lack of PI staining. Incubation with MRSA ± D-amino acids (D-Phe + D-Leu; 200 μM) induced widespread cell death (Fig. 5A), which was slightly reduced with lactisole compared to incubation with MRSA + D-amino acids alone (Fig. 5A, top row, quantified in Fig. 5B). However, addition of the T2R agonist denatonium resulted in fewer dead cells in cultures exposed to MRSA than did treatment with MRSA alone (Fig. 5A) likely because of AMPs secreted in response to denatonium activation of SCC T2Rs. The addition of D-amino acids exacerbated cell death under these conditions (Fig. 5, A and B), which was reversed by lactisole or gymnemic acid 2 (GA2) (Fig. 5A, middle row, quantified in Fig. 5B). This suggests that D-amino acid (DAA) activation of T1Rs inhibits the protective T2R-activated AMP response, reducing epithelial defense.

To demonstrate the relevance of this effect to clinically produced concentrations of D-amino acids, we tested the effects of MRSA strain M2 CM from 24-hour overnight cultures. MRSA CM blocked the pro-
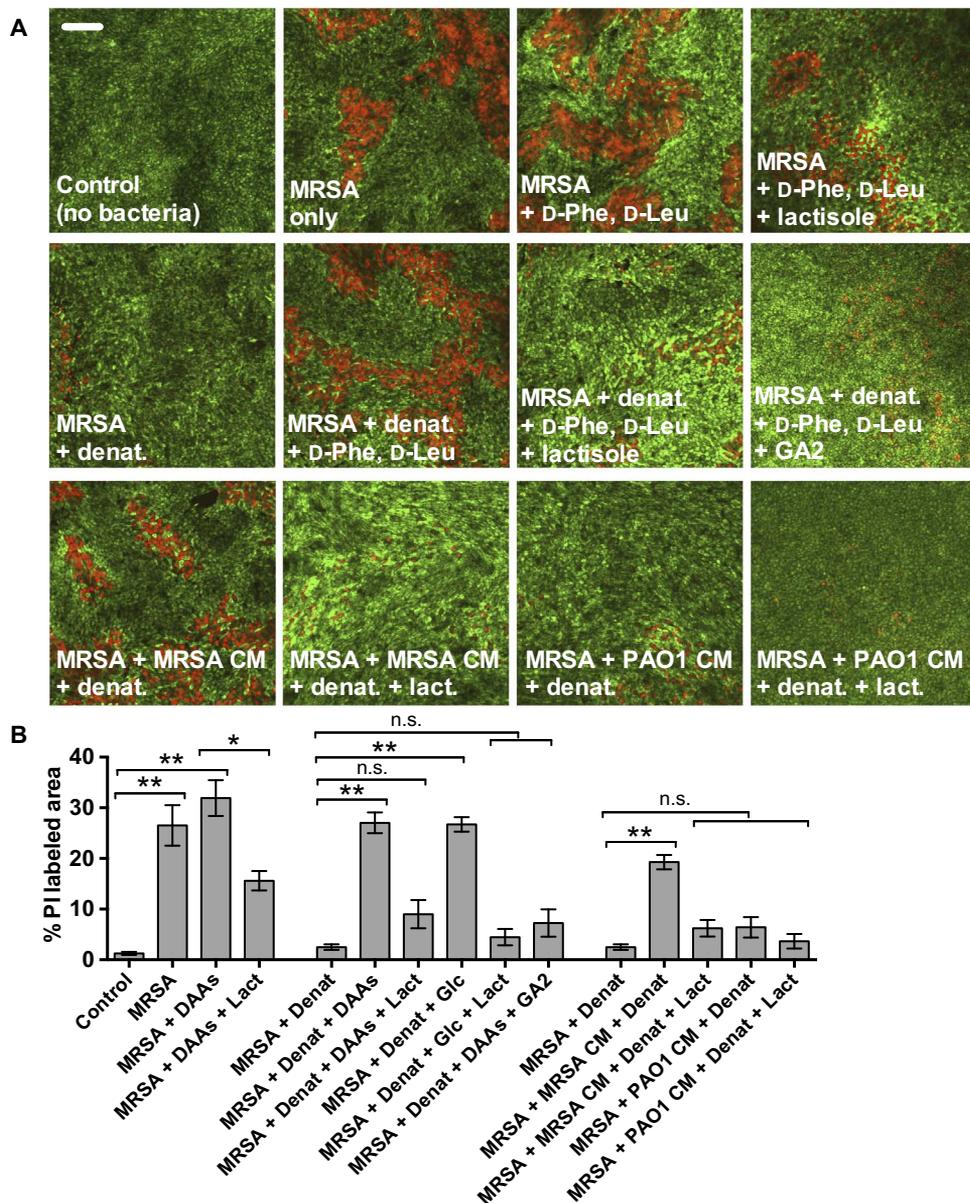

Fig. 5. Effects of D-amino acids on T2R-stimulated immune responses in vitro. (**A**) Representative images showing live cells labeled with Syto9 (green) and dead cells labeled with PI (red) in sinonasal ALI cultures after apical infection with MRSA in the presence or absence of D-Phe and D-Leu, lactisole, denatonium, GA2, MRSA CM, or PAO1 CM, as indicated. n = 3 to 6 independent experiments for each condition, each experiment averaging 10 fields of view from three ALI cultures from the same patient. Scale bar, 100 μm. (**B**) Data from experiments as in (A) and (B) quantified as % PI-stained area. n = 3 to 6 independent experiments (each from a different individual patient) for each condition, with each experiment averaging 10 fields of view from three ALI cultures from the same patient. Asterisks denote significance compared with the first bar of each graph (control conditions for that comparison) via one-way ANOVA with Dunnett's posttest; **P < 0.01. All graphs show means ± SEM (n = 4 to 6 patient ALI cultures for each condition).

tective effects of denatonium, resulting in cell death, but had no effect in the presence of lactisole (Fig. 5A, bottom row, quantified in Fig. 5B). Treatment of patient-derived ALI cultures with PAO1 CM had no effect (Fig. 5A, bottom row, quantified in Fig. 5B), suggesting that *Staphylococcus*, but not *Pseudomonas*, CM contains molecules, likely D-amino acids, that activate T1R to a level that reduces sinonasal innate immune responses by inhibiting AMP release.

DISCUSSION

The role of the T1R2/3 sweet taste receptor in sinonasal SCCs may have pathophysiological consequences in patients with diabetes mellitus, CRS, or cystic fibrosis, all of which have been reported to have increased ASL glucose concentrations (8, 30, 69–71). In control patients, nasal ASL glucose is low (<0.5 mM), which is similar to in vitro observations of ALI cultures grown in physiological (5 mM or 90 mg/dl) basolateral glucose (8). This amount of glucose only minimally attenuates SCC T2R responses. However, in patients with epithelial damage due to inflammatory disease, nasal ASL glucose is much higher (~1 to 2 mM), which significantly inhibits SCC T2R responses (8). Thus, increased ASL glucose secondary to disease may have inhibitory effects on epithelial innate immunity. Here, we show a further relevance of this mechanism to disease pathogenesis by demonstrating that sinonasal SCC T1R2/3 can be activated by bacterial D-amino acids. The data presented here show that clinically relevant respiratory Gram-positive *Staphylococcus* bacteria produce at least two T1R2/3-activating D-amino acids. Effects of D-amino acids may be magnified in combination with already high ASL glucose found in patients with sinonasal disease.

Because these D-amino acids have some effects on *P. aeruginosa*, this may be an important mechanism of bacterial cross-talk in the human airways. We found that D-amino acids were secreted by both *S. aureus* and *S. epidermidis*, which are generally considered to be nonpathogenic components of the normal respiratory flora (72). Although *S. aureus* plays an important role in CRS (73), it is considered an opportunistic pathogen because it is also a frequent colonizer of healthy sinuses (74–76). The secretion of D-amino acids may be a mechanism by which *Staphylococcus* strains suppress *P. aeruginosa* virulence, thus supporting a role for commensal *Staphylococcus* in preventing pathogenic growth of *P. aeruginosa* in the airways. Further studies are needed to understand whether this mechanism occurs at physiological concentrations of D-amino acids and whether it is involved in competition or growth coordination.

We also show that D-amino acids produced by *Staphylococcus* bacteria can suppress sinonasal SCC innate immune responses through activation of T1R and inhibition of AMP secretion. This may be a mechanism by which *Staphylococcus* species protect themselves from eradication and allow them to colonize human airways. More work is needed to determine whether the presence of D-amino acids in nasal mucus in infected patients is a potential biomarker of *Staphylococcus*-driven infections and whether T1R sweet receptor antagonists (for example, lactisole or gymnemic acid) are useful topical therapeutics in *S. aureus*–infected patients.

It has long been known that the innate and adaptive immune systems use pattern recognition receptors (PRRs) to detect conserved bacterial and viral components, such as Toll-like receptor 4 (TLR4)–mediated recognition of bacterial lipopolysaccharide (77). Our previous work (8, 14) and works of others (15–17) have demonstrated that T2Rs serve in an immune role similar to PRRs beyond their already established role on the tongue (25). The data here demonstrate that the T1R2/3 heterodimer also functions much like a PRR by recognizing bacterial D-amino acids, implicating D-amino acids in interkingdom signaling. However, in contrast to TLRs and T2Rs, activation of T1Rs suppresses innate immune responses. We do not yet know whether this provides a host benefit in vivo, for instance, in the prevention of activation of immune responses against commensal bacteria, or whether this is a mechanism by which pathogenic bacteria evade detection. One study has linked several *TAS1R* polymorphisms to increased risk of developing CRS (78). Because the sweet taste receptor has multiple ligand-binding sites (26), further research is needed to determine whether these polymorphisms affect the T1R response to D-amino acids. Because T1Rs are also present on other cell types throughout the body (11, 79), they may serve as PRR-like receptors that either suppress or stimulate innate immunity outside the airway.

MATERIALS AND METHODS

Reagents and solutions

Fluo-4 and LIVE/DEAD *Bac*Light Bacterial Viability Kit were purchased from Thermo Fisher Scientific. Lactisole (Cypha) was from Domino Foods Inc. Purified GA2 was from Four LLC. βD1 enzyme-linked immunosorbent assay development kit was from PeproTech, and the assay was carried out according to the manufacturer's instructions. Unless specified, all other reagents were from Sigma-Aldrich. Antibodies recognizing T1R2 (Abcam ab65417; RRID:AB_2200812) and T1R3 (Abcam ab65419; RRID:AB_1139947) for immunofluorescence, which were validated by Western blot in a previously published study (80) as well as in human embryonic kidney (HEK) 293T cells transfected with T1R2 or T1R3 (fig. S2), were used at 1:100. Antibody against T2R47 (Abcam ab65516; RRID:AB_1143241) was validated in our previous study (8). Antibody specific for β-tubulin IV was from Abcam (ab11315; RRID:AB_297919; mouse monoclonal; used at 1:250).

Phylogenetic tree construction

Evolutionary history was inferred using a maximum likelihood Jones-Taylor-Thornton (JTT) matrix–based model (81) on protein sequences obtained from GenBank and aligned with MUSCLE in MEGA6 (118 amino acid sequences; positions containing gaps and missing data were eliminated, resulting in 117 positions in the final data set) (82). The full highest log likelihood tree (−12115.8392) is shown in fig. S1. The percentage of trees in which the associated taxa clustered together is shown next to the branches. Initial tree(s) for the heuristic search was obtained by applying the neighbor-joining method to a matrix of pairwise distances estimated using a JTT model. Branch lengths reflect the number of substitutions per site.

Bacterial culture

Bacterial strains PAO1 (ATCC), MRSA M2 (83), ATCC 27853 (Boston 41501), PAO-GFP (gentamicin^r), and PAO-JP2 ($\Delta lasI$, $\Delta rhlI$; Tc^r, HgCl$_2$^{r}) (84, 85) were grown as previously described (8, 14). Patient sinonasal microbiology cultures were collected using the BBL CultureSwab Plus transport system (Becton Dickinson), grown overnight in lysogeny broth (LB) medium, and speciated by the Philadelphia Veterans Affairs Medical Center microbiological laboratory. Detection of D-amino acids from bacterial cultures was performed by the Children's Hospital of Philadelphia Metabolomics Core, using liquid chromatography followed by tandem mass spectrometry (LC-MS/MS) to detect D- and L-form stereo-isoforms of Phe, Leu, Ile, and Trp. Microbiological cultures isolated from human sinonasal swabs were grown for 24 hours at 37°C in LB medium, followed by normalization of turbidity to 0.5 McFarland. Sweet D-amino acid production was determined via LC-MS/MS.

Biofilm assays were performed using crystal violet staining in a 96-well plate, as previously described (86). Briefly, bacteria were normalized to 0.5 McFarland in LB medium or CM, and 100 μl was then aliquoted to 96-well plates containing 100 μl of 0.9% saline with the desired D- or L-amino acid(s) if applicable. Because of the poor solubility of Tyr, the maximum concentration of L-Tyr or D-Tyr in these experiments was 0.1 mM. In some assays, L-Phe and L-Leu or D-Phe and

D-Leu were increased above 0.1 mM as indicated in the figures, but the concentration of L-Tyr or D-Tyr was not increased beyond 0.1 mM. After incubation for 48 hours at 37°C, microtiter plates were washed three times with distilled water, followed by staining with 1% crystal violet for about 30 min at room temperature. After a second round of washing, biofilm mass and crystal violet were solubilized by incubation in 30% acetic acid for 30 min with shaking and read on a plate reader at 590 nm. Absorption spectra of bacterial culture supernatants were measured on a Tecan Spark 10M plate reader.

Pyocyanin extraction was carried out as previously described (87). Briefly, 8 ml of supernatant from an overnight culture (grown in cation-adjusted Mueller-Hinton broth, normalized to an optical density at 600 nm of 1) was mixed with 3 ml of chloroform. After vortexing and centrifugation, pyocyanin was extracted from the resulting organic chloroform phase with 1 ml of 0.2 N HCl, with absorbance of the acidified pyocyanin read at 520 nm in a plate reader (Bio-Rad). All values were blanked to the LB medium that had undergone the same extraction procedure. Relative concentrations of pyocyanin are shown because we are measuring relative inhibition and did not standardize to purified pyocyanin. However, raw pyocyanin concentrations can be estimated using the molar extinction coefficient of acidified pyocyanin [pyocyanin in micrograms per milliliter = $OD_{520} \times 17.072$ and pyocyanin molecular weight = 210.23, as previously described (87)]. Pyocyanin concentrations in PAO1 cultures grown to $OD_{600} = \sim1$ in peptone broth were previously reported to be ~60 μM (88). Here, we estimate pyocyanin in PAO1 cultures grown to $OD_{600} = 1$ in Mueller-Hinton broth to be 23 μM.

Bacterial swarming and swimming assays were performed as previously described (62, 89, 90). Plates contained (per 500 ml of M9 minimal medium) 1 g of glucose, 2.5 g of casamino acids, and 60 mg of $MgSO_4$ plus 1.5 g (0.3% final concentration) or 4 g (0.8% final concentration) of agar for swimming or swarming, respectively. Filter-sterilized solutions of L- or D-amino acids were added after autoclaving to prevent any heat-induced degradation. After spotting of 10 μl of bacteria (adjusted to $OD_{600} = 1$), plates were allowed to dry for 2 hours at room temperature and incubated overnight at 37°C. Antibacterial resistance tests were performed under the supervision of the Philadelphia Veterans Affairs Medical Center microbiological laboratory according to the procedures previously outlined in (91). Bacteria were normalized to 0.5 McFarland before plating on Mueller-Hinton agar plates coated with D- or L-amino acids (2 mM each in ddH2O applied with sterile swabs) before application of a broad spectrum of antibiotics against Gram-negative bacteria as indicated. Antibiotic resistance experiments were performed under the supervision of L. Chandler (director of the Philadelphia Veterans Affairs Medical Center Microbiology laboratory).

For microcolony dispersion assays, microcolonies were grown in Mattek glass-bottom dishes inoculated with PAO-GFP in LB medium + gentamicin and incubated for 48 hours at 37°C. Microcolonies (signifying the onset of biofilm formation) were visualized on a confocal microscope at a magnification of 60×; dispersion was induced by washing out the LB medium and replacing it with Hanks' balanced salt solution plus gentamicin (with glucose as the only nutrient source). Images were taken every 10 min over the course of several hours. Analysis was complicated by the fact that, once cells detached from the coverslip, they became motile and swam in and out of the field of view randomly; for this reason, raw fluorescence intensity or fluorescence area could not be used to quantify the number of cells remaining. A simple image processing workflow was used to measure only those static cells that were in the original first field of view. Image stacks (one time course of one field of view) were first converted to 8 bit,

and automatic thresholding was used to create a binary mask (background = 255, cells = 0) of the first image of the stack (time = 0) that was then applied to the entire image stack to minimize the contribution of cells swimming in and out of the image during the time course (that is, all fluorescence outside of the area of the original nonmotile cells was ignored). This allowed measurement of only those cells that were stuck to the coverslip in the first image. To minimize the effects (albeit minimal) of GFP photobleaching over time, we autothresholded the masked image at each time point to quantify the area of signal above background (proportional to the number of cells remaining on the coverslip) rather than the absolute fluorescence.

For determination of salt sensitivity, wild-type PAO1 *P. aeruginosa* was grown in LB medium overnight, followed by resuspension to 0.01 OD in normal saline at the concentrations indicated. Cells were incubated in low and normal salt solution for 2 hours, followed by dilution and spotting on LB agar plates (incubated overnight at 37°C) to count colony-forming units. All values were normalized to control (0.9% saline) values obtained within the same experiment (*n* = 3 to 4 experiments for each condition).

Human primary sinonasal epithelial ALI cell culture
Primary ALI cultures were set up as previously described (8, 14, 64, 92–94). Tissue was obtained from patients recruited from the Division of Rhinology, Department of Otorhinolaryngology—Head and Neck Surgery at the University of Pennsylvania and the Philadelphia Veterans Affairs Medical Center with informed consent and full approval of both Institutional Review Boards. Selection criteria for recruitment were patients undergoing sinonasal surgery. Exclusion criteria included a history of systemic diseases (for example, Wegner's, sarcoid, cystic fibrosis, and immunodeficiencies) and use of antibiotics, oral corticosteroids, or antibiologics (for example, Xolair) within 1 month of surgery. Enzymatically dissociated human sinonasal epithelial cells were grown to confluence in Dulbecco's modified Eagle's medium (DMEM)/Ham's F-12 and bronchial epithelial basal medium (BEBM; Clonetics, Cambrex) supplemented with penicillin (100 U/ml) and streptomycin (100 μg/ml) for 7 days. Cells were then trypsinized and seeded on porous polyester membranes in cell culture inserts (12 mm, 0.4-μm pores; Transwell-Clear, Corning) coated with 100 μl of coating solution [bovine serum albumin (BSA) (0.1 mg/ml), type I bovine collagen (30 μg/ml), and fibronectin (10 μg/ml) in LHC basal medium (Thermo Fisher Scientific)]. Five days later, the culture medium was removed from the upper compartment, and the epithelium was allowed to differentiate by using differentiation medium consisting of 1:1 DMEM (Thermo Fisher Scientific) and BEBM (Clonetics) with the Clonetics complements for human epidermal growth factor (0.5 ng/ml), epinephrine (5 μg/ml), bovine pituitary extract (0.13 mg/ml), hydrocortisone (0.5 μg/ml), insulin (5 μg/ml), triiodothyronine (6.5 μg/ml), and transferrin (0.5 μg/ml), supplemented with penicillin (100 UI/ml), streptomycin (100 g/ml), 0.1 nM retinoic acid, and 10% fetal bovine serum (FBS) in the basal compartment.

HEK293T cell culture and transfection
HEK293T cells (ATCC) were cultured in high-glucose DMEM (Gibco) with 10% FBS and 1× cell culture penicillin and streptomycin mix. Transfection for heterologous expression experiments was carried out with Lipofectamine 2000 according to the manufacturer's instructions using pcDNA3.1 vectors containing cloned sequences of human *TAS1R2* and *TAS1R3* cDNAs, with N-terminal rat somatostatin receptor 3 and C-terminal herpes simplex virus tags, as previously described

(28). Cells were fixed in 4% paraformaldehyde for 20 min and stained for immunofluorescence at 48 hours after transfection.

Immunofluorescence microscopy

Immunofluorescence of fixed HEK293T cells and ALI cultures was carried out as previously described (8, 14). Cells were fixed with 4% paraformaldehyde for 20 min at room temperature, followed by blocking and permeabilization for 1 hour in 0.25% saponin, 1% BSA, and 2% normal donkey serum. Antibodies directed against T1R2 and T1R3 were used with Molecular Probes' Zenon labeling kit for labeling of rabbit T1R2-directed and rabbit T1R3-directed antibodies. Images were viewed at magnifications of 20× (HEK293) or 60× (ALIs) on a wide-field inverted microscope (Olympus IX-83, 1.4 NA Plan Apo objective) running MetaMorph (Molecular Devices). After primary antibody incubation overnight at 4°C, secondary antibody incubation was performed for 2 hours at 4°C using Molecular Probes Alexa Fluor 488–conjugated donkey secondary antibody to detect β-tubulin IV. For HEK293T cell immunofluorescence, T1R2 and/or T1R3 rabbit polyclonal antibodies were used with mouse monoclonal FLAG-tag–directed antibody M2 (Sigma-Aldrich) or anti-hemagglutinin (16B12, ab130275). Donkey secondary antibodies directed against rabbit or mouse immunoglobulin G and conjugated to Alexa Fluor 488 or 555 were used to visualize primary antibody staining. Images were analyzed using MetaMorph, Fluoview software, and/or the FIJI (95) version of ImageJ (W. Rasband, Research Services Branch, National Institute of Mental Health).

Live-cell imaging of sinonasal ALI cultures

Fluo-4 loading and imaging were done exactly as previously described (8, 14, 92). Cells were loaded with 10 μM Fluo-4 AM (PBS + 0.1% pluronic F127; apical side only) for ~120 min at room temperature followed by three washes with Dulbecco's phosphate-buffered saline and 15- to 20-min incubation to allow cells to recover. Images were captured at 3- or 5-s intervals using the 488-nm laser line of an Olympus Fluoview confocal system attached to an Olympus IX81 microscope (10×, 0.3 NA UPlanFLN objective; Olympus). No gain, offset, or γ alterations were used. Normalization of Fluo-4 fluorescence changes was made after subtraction of background, approximated for each experiment by measuring unloaded ALIs. Baseline fluorescence (F_o) was determined by averaging the first 10 frames of each experiment.

Live/dead staining of ALIs was performed using Syto9/PI mix of a BacLight live/dead kit. MRSA M2 overnight cultures were centrifuged, normalized to 0.01 OD, and incubated with human ALI cultures for 6 hours at 37°C. Afterward, ALIs were washed copiously with PBS and stained using the two dyes at the concentrations indicated in the manufacturer's instructions and imaged immediately.

Data analyses and statistics

All statistical analyses were performed in GraphPad Prism; $P < 0.05$ was considered statistically significant. For multiple comparisons, ANOVA with Bonferroni posttest was used when preselected pairwise comparisons were performed, ANOVA with Tukey-Kramer posttest was used when all values in the data set were compared, and ANOVA with Dunnett's posttest was used when all values were compared with a control value. Tests used are indicated in the figure legends. For all figures, $*P < 0.05$, $**P < 0.01$, and n.s. indicates no statistical significance.

SUPPLEMENTARY MATERIALS

www.sciencesignaling.org/cgi/content/full/10/495/eaam7703/DC1

Fig. S1. Phylogenetic relationship of metabotropic glutamate receptor family proteins.

Fig. S2. Antibody validation in transfected HEK293 cells.

Fig. S3. Dispersion of PAO-GFP microcolonies in the presence or absence of D-amino acids.

Fig. S4. D-Amino acids did not affect salt sensitivity of *P. aeruginosa* strain PAO1.

Fig. S5. Sweet D-amino acids do not affect antibiotic sensitivity of PAO-GFP or ATCC 27853.

Fig. S6. D-Amino acid reduction of mouse nasal SCC T2R–stimulated Ca^{2+} signals requires T1R3.

Table S1. Sequences used for alignment for phylogenetic tree construction.

REFERENCES AND NOTES

1. B. M. Hariri, N. A. Cohen, New insights into upper airway innate immunity. *Am. J. Rhinol. Allergy* 30, 319–323 (2016).
2. J. L. Kennedy, L. Borish, Chronic rhinosinusitis and antibiotics: The good, the bad, and the ugly. *Am. J. Rhinol. Allergy* 27, 467–472 (2013).
3. R. A. Settipane, A. T. Peters, R. Chandra, Chapter 4: Chronic rhinosinusitis. *Am. J. Rhinol. Allergy* 27 (suppl. 1), S11–S15 (2013).
4. W. J. Fokkens, V. J. Lund, J. Mullol, C. Bachert, I. Alobid, F. Baroody, N. Cohen, A. Cervin, R. Douglas, P. Gevaert, C. Georgalas, H. Goossens, R. Harvey, P. Hellings, C. Hopkins, N. Jones, G. Joos, L. Kalogjera, B. Kern, M. Kowalski, D. Price, H. Riechelmann, R. Schlosser, B. Senior, M. Thomas, E. Toskala, R. Voegels, D. Y. Wang, P. J. Wormald, EPOS 2012: European position paper on rhinosinusitis and nasal polyps 2012. A summary for otorhinolaryngologists. *Rhinol.* 3, 1–298 (2012).
5. J. Marcinkiewicz, M. Strus, E. Pasich, Antibiotic resistance: A "dark side" of biofilm–associated chronic infections. *Pol. Arch. Med. Wewn.* 123, 309–313 (2013).
6. V. Rujanavej, E. Soudry, N. Banaei, E. J. Baron, P. H. Hwang, J. V. Nayak, Trends in incidence and susceptibility among methicillin-resistant *Staphylococcus aureus* isolated from intranasal cultures associated with rhinosinusitis. *Am. J. Rhinol. Allergy* 27, 134–137 (2013).
7. R. P. Manes, P. S. Batra, Bacteriology and antibiotic resistance in chronic rhinosinusitis. *Facial Plast. Surg. Clin. North Am.* 20, 87–91 (2012).
8. R. J. Lee, J. M. Kofonow, P. L. Rosen, A. P. Siebert, B. Chen, L. Doghramji, G. Xiong, N. D. Adappa, J. N. Palmer, D. W. Kennedy, J. L. Kreindler, R. F. Margolskee, N. A. Cohen, Bitter and sweet taste receptors regulate human upper respiratory innate immunity. *J. Clin. Invest.* 124, 1393–1405 (2014).
9. R. F. Margolskee, Teaching resources. Sensory systems: Taste perception. *Sci. STKE* 2005, tr20 (2005).
10. R. F. Margolskee, The molecular biology of taste transduction. *Bioessays* 15, 645–650 (1993).
11. A. Laffitte, F. Neiers, L. Briand, Functional roles of the sweet taste receptor in oral and extraoral tissues. *Curr. Opin. Clin. Nutr. Metab. Care* 17, 379–385 (2014).
12. I. Depoortere, Taste receptors of the gut: Emerging roles in health and disease. *Gut* 63, 179–190 (2014).
13. R. J. Lee, N. A. Cohen, Taste receptors in innate immunity. *Cell. Mol. Life Sci.* 72, 217–236 (2015).
14. R. J. Lee, G. Xiong, J. M. Kofonow, B. Chen, A. Lysenko, P. Jiang, V. Abraham, L. Doghramji, N. D. Adappa, J. N. Palmer, D. W. Kennedy, G. K. Beauchamp, P.-T. Doulias, H. Ischiropoulos, J. L. Kreindler, D. R. Reed, N. A. Cohen, T2R38 taste receptor polymorphisms underlie susceptibility to upper respiratory infection. *J. Clin. Invest.* 122, 4145–4159 (2012).
15. K. Deckmann, K. Filipski, G. Krasteva-Christ, M. Fronius, M. Althaus, A. Rafiq, T. Papadakis, L. Renno, I. Jurastow, L. Wessels, M. Wolff, B. Schütz, E. Weihe, V. Chubanov, T. Gudermann, J. Klein, T. Bschleipfer, W. Kummer, Bitter triggers acetylcholine release from polymodal urethral chemosensory cells and bladder reflexes. *Proc. Natl. Acad. Sci. U.S.A.* 111, 8287–8292 (2014).
16. S. Maurer, G. H. Wabnitz, N. A. Kahle, S. Stegmaier, B. Prior, T. Giese, M. M. Gaida, Y. Samstag, G. M. Hänsch, Tasting *Pseudomonas aeruginosa* biofilms: Human neutrophils express the bitter receptor T2R38 as sensor for the quorum sensing molecule *N*-(3-oxododecanoyl)-L-homoserine lactone. *Front. Immunol.* 6, 369 (2015).
17. M. Tizzano, B. D. Gulbransen, A. Vandenbeuch, T. R. Clapp, J. P. Herman, H. M. Sibhatu, M. E. A. Churchill, W. L. Silver, S. C. Kinnamon, T. E. Finger, Nasal chemosensory cells use bitter taste signaling to detect irritants and bacterial signals. *Proc. Natl. Acad. Sci. U.S.A.* 107, 3210–3215 (2010).
18. C. J. Saunders, M. Christensen, T. E. Finger, M. Tizzano, Cholinergic neurotransmission links solitary chemosensory cells to nasal inflammation. *Proc. Natl. Acad. Sci. U.S.A.* 111, 6075–6080 (2014).
19. T. E. Finger, Evolution of taste and solitary chemoreceptor cell systems. *Brain Behav. Evol.* 50, 234–243 (1997).
20. A. Hansen, Olfactory and solitary chemosensory cells: Two different chemosensory systems in the nasal cavity of the American alligator, *Alligator mississippiensis*. *BMC Neurosci.* 8, 64 (2007).
21. M. Tizzano, M. Cristofoletti, A. Sbarbati, T. E. Finger, Expression of taste receptors in solitary chemosensory cells of rodent airways. *BMC Pulm. Med.* 11, 3 (2011).

22. B. D. Gulbransen, T. R. Clapp, T. E. Finger, S. C. Kinnamon, Nasal solitary chemoreceptor cell responses to bitter and trigeminal stimulants in vitro. *J. Neurophysiol.* **99**, 2929–2937 (2008).

23. T. E. Finger, B. Böttger, A. Hansen, K. T. Anderson, H. Alimohammadi, W. L. Silver, Solitary chemoreceptor cells in the nasal cavity serve as sentinels of respiration. *Proc. Natl. Acad. Sci. U.S.A.* **100**, 8981–8986 (2003).

24. H. P. Barham, S. E. Cooper, C. B. Anderson, M. Tizzano, T. T. Kingdom, T. E. Finger, S. C. Kinnamon, V. R. Ramakrishnan, Solitary chemosensory cells and bitter taste receptor signaling in human sinonasal mucosa. *Int. Forum Allergy Rhinol.* **3**, 450–457 (2013).

25. R. F. Margolskee, Molecular mechanisms of bitter and sweet taste transduction. *J. Biol. Chem.* **277**, 1–4 (2002).

26. M. Cui, P. Jiang, E. Maillet, M. Max, R. F. Margolskee, R. Osman, The heterodimeric sweet taste receptor has multiple potential ligand binding sites. *Curr. Pharm. Des.* **12**, 4591–4600 (2006).

27. P. Jiang, M. Cui, B. Zhao, Z. Liu, L. A. Snyder, L. M. J. Benard, R. Osman, R. F. Margolskee, M. Max, Lactisole interacts with the transmembrane domains of human T1R3 to inhibit sweet taste. *J. Biol. Chem.* **280**, 15238–15246 (2005).

28. P. Jiang, M. Cui, B. Zhao, L. A. Snyder, L. M. J. Benard, R. Osman, M. Max, R. F. Margolskee, Identification of the cyclamate interaction site within the transmembrane domain of the human sweet taste receptor subunit T1R3. *J. Biol. Chem.* **280**, 34296–34305 (2005).

29. T. Imada, T. Misaka, S. Fujiwara, S. Okada, Y. Fukuda, K. Abe, Amiloride reduces the sweet taste intensity by inhibiting the human sweet taste receptor. *Biochem. Biophys. Res. Commun.* **397**, 220–225 (2010).

30. J. P. Garnett, E. H. Baker, D. L. Baines, Sweet talk: Insights into the nature and importance of glucose transport in lung epithelium. *Eur. Respir. J.* **40**, 1269–1276 (2012).

31. K. K. Kalsi, E. H. Baker, O. Fraser, Y.-L. Chung, O. J. Mace, E. Tarelli, B. J. Philips, D. L. Baines, Glucose homeostasis across human airway epithelial cell monolayers: Role of diffusion, transport and metabolism. *Pflugers Arch.* **457**, 1061–1070 (2009).

32. A. A. Pezzulo, J. Gutiérrez, K. S. Duschner, K. S. McConnell, P. J. Taft, S. E. Ernst, T. L. Yahr, K. Rahmouni, J. Klesney-Tait, D. A. Stoltz, J. Zabner, Glucose depletion in the airway surface liquid is essential for sterility of the airways. *PLOS ONE* **6**, e16166 (2011).

33. A. Bassoli, G. Borgonovo, F. Caremoli, G. Mancuso, The taste of D- and L-amino acids: In vitro binding assays with cloned human bitter (TAS2Rs) and sweet (TAS1R2/TAS1R3) receptors. *Food Chem.* **150**, 27–33 (2014).

34. G. Zhang, H. J. Sun, Racemization in reverse: Evidence that D-amino acid toxicity on Earth is controlled by bacteria with racemases. *PLOS ONE* **9**, e92101 (2014).

35. H. Lam, D.-C. Oh, F. Cava, C. N. Takacs, J. Clardy, M. A. de Pedro, M. K. Waldor, D-Amino acids govern stationary phase cell wall remodeling in bacteria. *Science* **325**, 1552–1555 (2009).

36. I. Kolodkin-Gal, D. Romero, S. Cao, J. Clardy, R. Kolter, R. Losick, D-Amino acids trigger biofilm disassembly. *Science* **328**, 627–629 (2010).

37. K. S. Brandenburg, K. J. Rodriguez, J. F. McAnulty, C. J. Murphy, N. L. Abbott, M. J. Schurr, C. J. Czuprynski, Tryptophan inhibits biofilm formation by *Pseudomonas aeruginosa*. *Antimicrob. Agents Chemother.* **57**, 1921–1925 (2013).

38. C. Yu, J. Wu, A. E. Contreras, Q. Li, Control of nanofiltration membrane biofouling by *Pseudomonas aeruginosa* using D-tyrosine. *J. Membr. Sci.* **423–424**, 487–494 (2012).

39. A. J. Harmata, Y. Ma, C. J. Sanchez, K. J. Zienkiewicz, F. Elefteriou, J. C. Wenke, S. A. Guelcher, D-Amino acid inhibits biofilm but not new bone formation in an ovine model. *Clin. Orthop. Relat. Res.* **473**, 3951–3961 (2015).

40. A. I. Hochbaum, I. Kolodkin-Gal, L. Foulston, R. Kolter, J. Aizenberg, R. Losick, Inhibitory effects of D-amino acids on *Staphylococcus aureus* biofilm development. *J. Bacteriol.* **193**, 5616–5622 (2011).

41. M. L. Ramón-Peréz, F. Diaz-Cedillo, J. A. Ibarra, A. Torales-Cardeña, S. Rodríguez-Martínez, J. Jan-Roblero, M. E. Cancino-Diaz, J. C. Cancino-Diaz, D-Amino acids inhibit biofilm formation in *Staphylococcus epidermidis* strains from ocular infections. *J. Med. Microbiol.* **63**, 1369–1376 (2014).

42. C. J. Sanchez Jr., K. S. Akers, D. R. Romano, R. L. Woodbury, S. K. Hardy, C. K. Murray, J. C. Wenke, D-Amino acids enhance the activity of antimicrobials against biofilms of clinical wound isolates of *Staphylococcus aureus* and *Pseudomonas aeruginosa*. *Antimicrob. Agents Chemother.* **58**, 4353–4361 (2014).

43. H. Xu, Y. Liu, D-Amino acid mitigated membrane biofouling and promoted biofilm detachment. *J. Membr. Sci.* **376**, 266–275 (2011).

44. H. Xua, Y. Liu, Reduced microbial attachment by D-amino acid-inhibited AI-2 and EPS production. *Water Res.* **45**, 5796–5804 (2011).

45. S.-F. Xing, X.-F. Sun, A. A. Taylor, S. L. Walker, Y.-F. Wang, S.-G. Wang, D-Amino acids inhibit initial bacterial adhesion: Thermodynamic evidence. *Biotechnol. Bioeng.* **112**, 696–704 (2015).

46. J. Yang, J. Yu, J. Jiang, C. Liang, Y. Feng, D-tyrosine affects aggregation behavior of Pantoea agglomerans. *J. Basic Microbiol.* **57**, 184–189 (2016).

47. S. Sarkar, M. M. Pires, D-Amino acids do not inhibit biofilm formation in *Staphylococcus aureus*. *PLOS ONE* **10**, e0117613 (2015).

48. S. A. Leiman, J. M. May, M. D. Lebar, D. Kahne, R. Kolter, R. Losick, D-Amino acids indirectly inhibit biofilm formation in *Bacillus subtilis* by interfering with protein synthesis. *J. Bacteriol.* **195**, 5391–5395 (2013).

49. Y. Li, R. Jia, H. H. Al-Mahamedh, D. Xu, T. Gu, Enhanced biocide mitigation of field biofilm consortia by a mixture of D-Amino acids. *Front. Microbiol.* **7**, 896 (2016).

50. P. She, L. Chen, H. Liu, Y. Zou, Z. Luo, A. Koronfel, Y. Wu, The effects of D-Tyrosine combined with amikacin on the biofilms of *Pseudomonas aeruginosa*. *Microb. Pathog.* **86**, 38–44 (2015).

51. C. Yu, X. Li, N. Zhang, D. Wen, C. Liu, Q. Li, Inhibition of biofilm formation by D-tyrosine: Effect of bacterial type and D-tyrosine concentration. *Water Res.* **92**, 173–179 (2016).

52. F. Cava, H. Lam, M. A. de Pedro, M. K. Waldor, Emerging knowledge of regulatory roles of D-amino acids in bacteria. *Cell. Mol. Life Sci.* **68**, 817–831 (2011).

53. R. S. Shallenberger, T. E. Acree, C. Y. Lee, Sweet taste of D and L-sugars and amino-acids and the steric nature of their chemo-receptor site. *Nature* **221**, 555–556 (1969).

54. T. K. Bjarnadóttir, R. Fredriksson, H. B. Schiöth, The gene repertoire and the common evolutionary history of glutamate, pheromone (V2R), taste(1) and other related G protein-coupled receptors. *Gene* **362**, 70–84 (2005).

55. N. Nuemket, N. Yasui, Y. Kusakabe, Y. Nomura, N. Atsumi, S. Akiyama, E. Nango, Y. Kato, M. K. Kaneko, J. Takagi, M. Hosotani, A. Yamashita, Structural basis for perception of diverse chemical substances by T1r taste receptors. *Nat. Commun.* **8**, 15530 (2017).

56. J. A. Morris, R. Martenson, G. Deibler, R. H. Cagan, Characterization of monellin, a protein that tastes sweet. *J. Biol. Chem.* **248**, 534–539 (1973).

57. M. Tizzano, T. E. Finger, Chemosensors in the nose: Guardians of the airways. *Physiology (Bethesda)* **28**, 51–60 (2013).

58. R. J. Lee, N. A. Cohen, Sinonasal solitary chemosensory cells "taste" the upper respiratory environment to regulate innate immunity. *Am. J. Rhinol. Allergy* **28**, 366–373 (2014).

59. S. S. Schiffman, K. Sennewald, J. Gagnon, Comparison of taste qualities and thresholds of D- and L-amino acids. *Physiol. Behav.* **27**, 51–59 (1981).

60. J. Solms, L. Vuataz, R. H. Egli, The taste of L- and D-amino acids. *Experientia* **21**, 692–694 (1965).

61. M. Kawai, Y. Sekine-Hayakawa, A. Okiyama, Y. Ninomiya, Gustatory sensation of L- and D-amino acids in humans. *Amino Acids* **43**, 2349–2358 (2012).

62. D.-G. Ha, S. L. Kuchma, G. A. O'Toole, Plate-based assay for swarming motility in *Pseudomonas aeruginosa*. *Methods Mol. Biol.* **1149**, 67–72 (2014).

63. N. C. Caiazza, R. M. Q. Shanks, G. A. O'Toole, Rhamnolipids modulate swarming motility patterns of *Pseudomonas aeruginosa*. *J. Bacteriol.* **187**, 7351–7361 (2005).

64. Y. Lai, B. Chen, J. Shi, J. N. Palmer, D. W. Kennedy, N. A. Cohen, Inflammation-mediated upregulation of centrosomal protein 110, a negative modulator of ciliogenesis, in patients with chronic rhinosinusitis. *J. Allergy Clin. Immunol.* **128**, 1207–1215.e1 (2011).

65. R. J. Lee, N. A. Cohen, Bitter and sweet taste receptors in the respiratory epithelium in health and disease. *J. Mol. Med.* **92**, 1235–1244 (2014).

66. S. Dimova, M. E. Brewster, M. Noppe, M. Jorissen, P. Augustijns, The use of human nasal in vitro cell systems during drug discovery and development. *Toxicol. In Vitro* **19**, 107–122 (2005).

67. K. Sanematsu, Y. Kusakabe, N. Shigemura, T. Hirokawa, S. Nakamura, T. Imoto, Y. Ninomiya, Molecular mechanisms for sweet-suppressing effect of gymnemic acids. *J. Biol. Chem.* **289**, 25711–25720 (2014).

68. H. L. Meiselman, B. P. Halpern, Effects of Gymnema sylvestre on complex tastes elicited by amino acids and sucrose. *Physiol. Behav.* **5**, 1379–1384 (1970).

69. S. K. Gill, K. Hui, H. Farne, J. P. Garnett, D. L. Baines, L. S. P. Moore, A. H. Holmes, A. Filloux, J. S. Tregoning, Increased airway glucose increases airway bacterial load in hyperglycaemia. *Sci. Rep.* **6**, 27636 (2016).

70. J. P. Garnett, T. T. Nguyen, J. D. Moffatt, E. R. Pelham, K. K. Kalsi, E. H. Baker, D. L. Baines, Proinflammatory mediators disrupt glucose homeostasis in airway surface liquid. *J. Immunol.* **189**, 373–380 (2012).

71. E. H. Baker, N. Clark, A. L. Brennan, D. A. Fisher, K. M. Gyi, M. E. Hodson, B. J. Philips, D. L. Baines, D. M. Wood, Hyperglycemia and cystic fibrosis alter respiratory fluid glucose concentrations estimated by breath condensate analysis. *J. Appl. Physiol.* **102**, 1969–1975 (2007).

72. T. T. Rasmussen, L. P. Kirkeby, K. Poulsen, J. Reinholdt, M. Kilian, Resident aerobic microbiota of the adult human nasal cavity. *APMIS* **108**, 663–675 (2000).

73. D. L. Hamilos, Host-microbial interactions in patients with chronic rhinosinusitis. *J. Allergy Clin. Immunol.* **133**, 640–653.e4 (2014).

74. K. Sivaraman, N. Venkataraman, A. M. Cole, *Staphylococcus aureus* nasal carriage and its contributing factors. *Future Microbiol.* **4**, 999–1008 (2009).

75. P. O. Verhoeven, J. Gagnaire, E. Botelho-Nevers, F. Grattard, A. Carricajo, F. Lucht, B. Pozzetto, P. Berthelot, Detection and clinical relevance of *Staphylococcus aureus* nasal carriage: An update. *Expert Rev. Anti Infect. Ther.* **12**, 75–89 (2014).

76. B. Krismer, A. Peschel, Does *Staphylococcus aureus* nasal colonization involve biofilm formation? *Future Microbiol.* **6**, 489–493 (2011).

77. A. Muir, G. Soong, S. Sokol, B. Reddy, M. I. Gomez, A. Van Heeckeren, A. Prince, Toll-like receptors in normal and cystic fibrosis airway epithelial cells. *Am. J. Respir. Cell Mol. Biol.* **30**, 777–783 (2004).

78. L. Mfuna Endam, A. Filali-Mouhim, P. Boisvert, L. P. Boulet, Y. Bossé, M. Desrosiers, Genetic variations in taste receptors are associated with chronic rhinosinusitis: A replication study. *Int. Forum Allergy Rhinol.* **4**, 200–206 (2014).

79. A. C. Meyer-Gerspach, B. Wolnerhanssen, C. Beglinger, Gut sweet taste receptors and their role in metabolism. *Front. Horm. Res.* **42**, 123–133 (2014).

80. R. A. Elliott, S. Kapoor, D. G. Tincello, Expression and distribution of the sweet taste receptor isoforms T1R2 and T1R3 in human and rat bladders. *J. Urol.* **186**, 2455–2462 (2011).

81. D. T. Jones, W. R. Taylor, J. M. Thornton, The rapid generation of mutation data matrices from protein sequences. *Comput. Appl. Biosci.* **8**, 275–282 (1992).

82. K. Tamura, G. Stecher, D. Peterson, A. Filipski, S. Kumar, MEGA6: Molecular evolutionary genetics analysis version 6.0. *Mol. Biol. Evol.* **30**, 2725–2729 (2013).

83. M. E. Shirtliff, J. H. Calhoun, J. T. Mader, Experimental osteomyelitis treatment with antibiotic-impregnated hydroxyapatite. *Clin. Orthop. Relat. Res.*, 239–247 (2002).

84. J. P. Pearson, K. M. Gray, L. Passador, K. D. Tucker, A. Eberhard, B. H. Iglewski, E. P. Greenberg, Structure of the autoinducer required for expression of *Pseudomonas aeruginosa* virulence genes. *Proc. Natl. Acad. Sci. U.S.A.* **91**, 197–201 (1994).

85. J. P. Pearson, E. C. Pesci, B. H. Iglewski, Roles of *Pseudomonas aeruginosa* las and rhl quorum-sensing systems in control of elastase and rhamnolipid biosynthesis genes. *J. Bacteriol.* **179**, 5756–5767 (1997).

86. G. A. O'Toole, Microtiter dish biofilm formation assay. *J. Vis. Exp.* **30**, 2437 (2011).

87. D. W. Essar, L. Eberly, A. Hadero, I. P. Crawford, Identification and characterization of genes for a second anthranilate synthase in *Pseudomonas aeruginosa*: Interchangeability of the two anthranilate synthases and evolutionary implications. *J. Bacteriol.* **172**, 884–900 (1990).

88. B. R. Lundgren, W. Thornton, M. H. Dornan, L. R. Villegas-Peñaranda, C. N. Boddy, C. T. Nomura, Gene PA2449 is essential for glycine metabolism and pyocyanin biosynthesis in Pseudomonas aeruginosa PAO1. *J. Bacteriol.* **195**, 2087–2100 (2013).

89. D.-G. Ha, S. L. Kuchma, G. A. O'Toole, Plate-based assay for swimming motility in *Pseudomonas aeruginosa*. *Methods Mol. Biol.* **1149**, 59–65 (2014).

90. B. M. Hariri, S. J. Payne, B. Chen, C. Mansfield, L. J. Doghramji, N. D. Adappa, J. N. Palmer, D. W. Kennedy, M. Y. Niv, R. J. Lee, In vitro effects of anthocyanidins on sinonasal epithelial nitric oxide production and bacterial physiology. *Am. J. Rhinol. Allergy* **30**, 261–268 (2016).

91. J. Hindler, in *Clinical Microbiology Procedures Handbook*, H. D. Isenberg, Ed. (ASM Press, ed. 2, 2005).

92. R. J. Lee, B. Chen, L. Doghramji, N. D. Adappa, J. N. Palmer, D. W. Kennedy, N. A. Cohen, Vasoactive intestinal peptide regulates sinonasal mucociliary clearance and synergizes with histamine in stimulating sinonasal fluid secretion. *FASEB J.* **27**, 5094–5103 (2013).

93. K.-Q. Zhao, A. T. Cowan, R. J. Lee, N. Goldstein, K. Droguett, B. Chen, C. Zheng, M. Villalon, J. N. Palmer, J. L. Kreindler, N. A. Cohen, Molecular modulation of airway epithelial ciliary response to sneezing. *FASEB J.* **26**, 3178–3187 (2012).

94. B. M. Hariri, D. B. McMahon, B. Chen, J. R. Freund, C. J. Mansfield, L. J. Doghramji, N. D. Adappa, J. N. Palmer, D. W. Kennedy, D. R. Reed, P. Jiang, R. J. Lee, Flavones modulate respiratory epithelial innate immunity: Anti-inflammatory effects and activation of the T2R14 receptor. *J. Biol. Chem.* **292**, 8484–8497 (2017).

95. J. Schindelin, I. Arganda-Carreras, E. Frise, V. Kaynig, M. Longair, T. Pietzsch, S. Preibisch, C. Rueden, S. Saalfeld, B. Schmid, J.-Y. Tinevez, D. J. White, V. Hartenstein, K. Eliceiri, P. Tomancak, A. Cardona, Fiji: An open-source platform for biological-image analysis. *Nat. Methods* **9**, 676–682 (2012).

Citation: R. J. Lee, B. M. Hariri, D. B. McMahon, B. Chen, L. Doghramji, N. D. Adappa, J. N. Palmer, D. W. Kennedy, P. Jiang, R. F. Margolskee, N. A. Cohen, Bacterial D-amino acids suppress sinonasal innate immunity through sweet taste receptors in solitary chemosensory cells. *Sci. Signal.* **10**, eaam7703 (2017).

Science Signaling

Bacterial d-amino acids suppress sinonasal innate immunity through sweet taste receptors in solitary chemosensory cells

Robert J. Lee, Benjamin M. Hariri, Derek B. McMahon, Bei Chen, Laurel Doghramji, Nithin D. Adappa, James N. Palmer, David W. Kennedy, Peihua Jiang, Robert F. Margolskee and Noam A. Cohen

The sweet taste of bacteria

Stimulation of the sweet taste receptor (T1R) in solitary chemosensory cells of the upper respiratory epithelium inhibits the release of antimicrobial peptides by neighboring epithelial cells. In addition to being activated by various sugars, T1R can also be activated by some d-amino acids. Lee *et al.* found that *Staphylococcus* species in the nasal cavities of chronic rhinosinusitis patients produced d-Phe and d-Leu, both of which can activate T1R. Treatment of primary human sinonasal epithelial cultures with d-Phe and d-Leu inhibited the release of antimicrobial peptides and increased cell death in response to infection with methicillin-resistant *S. aureus*. d-Phe and d-Leu, as well as medium conditioned by respiratory isolates of *Staphylococcus*, inhibited the formation of *Pseudomonas aeruginosa* biofilms. These findings demonstrate that d-amino acids produced by nasal flora can inhibit innate immune responses through T1R and may shape the microbial community of the airways.

ARTICLE TOOLS	http://stke.sciencemag.org/content/10/495/eaam7703
SUPPLEMENTARY MATERIALS	http://stke.sciencemag.org/content/suppl/2017/08/31/10.495.eaam7703.DC1
RELATED CONTENT	http://stke.sciencemag.org/content/sigtrans/8/370/fs6.full http://stke.sciencemag.org/content/sigtrans/8/372/ra36.full http://stm.sciencemag.org/content/scitransmed/9/376/eaaf9412.full http://science.sciencemag.org/content/sci/351/6279/1329.full http://stke.sciencemag.org/content/sigtrans/10/496/eaap8920.full http://stke.sciencemag.org/content/sigtrans/10/496/eaap9099.full http://stke.sciencemag.org/content/sigtrans/10/496/eaap8921.full http://stke.sciencemag.org/content/sigtrans/10/501/eaan4893.full http://stke.sciencemag.org/content/sigtrans/10/508/eaar6316.full http://stm.sciencemag.org/content/scitransmed/9/378/eaah4680.full http://stke.sciencemag.org/content/sigtrans/11/532/eaau2601.full http://stke.sciencemag.org/content/sigtrans/12/612/eaba5393.full
REFERENCES	This article cites 93 articles, 25 of which you can access for free http://stke.sciencemag.org/content/10/495/eaam7703#BIBL
PERMISSIONS	http://www.sciencemag.org/help/reprints-and-permissions

Use of this article is subject to the Terms of Service